Peiming Zheng, Takaaki Ito, Dan Aoki*, Saori Sato, Masato Yoshida, Yuzou Sano, Yasuyuki Matsushita, Kazuhiko Fukushima and Kumi Yoshida*

Determination of inorganic element distribution in the freeze-fixed stem of $Al_2(SO_4)_3$-treated *Hydrangea macrophylla* by TOF-SIMS and ICP-AES

DOI 10.1515/hf-2016-0149
Received September 14, 2016; accepted February 27, 2017; previously published online March 30, 2017

Abstract: To elucidate the effect of soil conditions on the *in planta* distribution of inorganic elements, an aluminium (Al)-tolerant plant, *Hydrangea macrophylla*, was cultivated with the addition of Al ion to soils. Freeze-dried stems from the plants were analysed by time-of-flight secondary ion mass spectrometry (dry-TOF-SIMS). Freeze-fixed stems of the plants were analysed by cryo-TOF-SIMS. The inorganic metal content was quantified by inductively coupled plasma atomic absorption spectrometry (ICP-AES). The dry- and cryo-TOF-SIMS mapping analyses showed that in the native sample, inorganic elements are mainly localised in the cortex and pith. Al-treatment [i.e. $Al_2(SO_4)_3$ administration to the soil] altered the distribution and content of inorganic metals. The actual amount of inorganic elements quantified by ICP-AES showed that Al-treatment on the soil increased the amounts of Na, Mg, Al and Ca and decreased that of K in the stem. The secondary ion counts of inorganic elements in freeze-dried and -fixed samples, determined by dry-/cryo-TOF-SIMS measurements, showed similar variations as that observed with ICP-AES measurements. These results are interpreted as that Al-treatment altered the distribution and amount of inorganic elements in the stems of Al-tolerant *H. macrophylla* plants.

Keywords: aluminium tolerance, *Hydrangea macrophylla*, inductively coupled plasma atomic emission spectrometry (ICP-AES), inorganic element, time-of-flight secondary ion mass spectrometry (TOF-SIMS)

***Corresponding authors: Dan Aoki,** Graduate School of Bioagricultural Sciences, Nagoya University, Chikusa-ku, Nagoya 464-8601, Japan, Phone: +81-52-789-4062, Fax: +81-52-789-4163, e-mail: daoki@agr.nagoya-u.ac.jp; and **Kumi Yoshida,** Graduate School of information Science, Nagoya University, Chikusa-ku, Nagoya 464-8601, Japan, Phone: +81-52-789-5638, Fax: +81-52-789-5638, e-mail: yoshidak@is.nagoya-u.ac.jp
Peiming Zheng: Graduate School of Bioagricultural Sciences, Nagoya University, Nagoya, Japan; and School of Life Science, Shandong University, Jinan, China
Takaaki Ito: Graduate School of information Science, Nagoya University, Nagoya, Japan
Saori Sato, Masato Yoshida, Yasuyuki Matsushita and Kazuhiko Fukushima: Graduate School of Bioagricultural Sciences, Nagoya University, Nagoya, Japan
Yuzou Sano: Research Faculty of Agriculture, Hokkaido University, Sapporo, Japan

Introduction

Aluminium (Al) toxicity is a major growth-limiting factor in plants worldwide, especially in acid soils (Siegel 1985; Horst 1995; Kochian 1995; Matsumoto 2000; Samac and Tesfaye 2003; Kochian et al. 2004; Ma 2007). Because acidic soils comprise up to 40% of the world's potentially arable lands (Vonuexkull and Mutert 1995), an important task in agricultural and plant physiological research is breeding of crops tolerant to Al-toxicity (Horst 1995; Kochian 1995; Ma et al. 1997, 2001; Matsumoto 2000; Samac and Tesfaye 2003; Kochian et al. 2004; Ma 2007; Famoso et al. 2010). Al ions in acidic soils rapidly inhibit root-cell elongation and reduce root surface area, which impedes most nutrient accumulation (Kochian 1995; Rufty et al. 1995; Matsumoto 2000; Rout et al. 2001; Kochian et al. 2004; Ma 2007). In addition, owing to direct Al interference with the efficiency of membrane-transport mechanisms, other inorganic elements such as Ca and Mg also showed lowered internal concentrations in the plant, thereby affecting plant growth (Siegel 1985; Horst 1995; Kochian 1995; Matsumoto 2000; Samac and Tesfaye 2003; Kochian et al. 2004; Ma 2007). Despite Al phytotoxicity, some plant species such as *Fagopyrum esculentum* (Moench) (Shen et al. 2006), *Camellia sinensis* (L.) Kuntze (Hajiboland et al. 2013), *Hydrangea macrophylla* (Thunb.) Ser. (Ma et al. 1997, 2001; Toyama-Kato et al. 2003; Ito et al. 2009), *Melastoma malabathricum* (L.) (Watanabe et al. 2008a,b) and *Arbor aluminosa* (Schmitt et al. 2016) can accumulate Al at high concentrations without showing any signs of toxicity. Several of these species growing in acid soil can accumulate Al up to concentrations >1000 mg kg^{-1} on a dry-weight (DW) basis

(Ma et al. 1997; Hajiboland et al. 2013; Schmitt et al. 2016). However, to our knowledge, limited studies have examined the microscopic distribution of inorganic elements in plant species affected by Al-rich conditions.

Time-of-flight secondary ion mass spectrometry (TOF-SIMS) is an analytical technique that has high mass and spatial resolution and provides information on the chemical features of the surfaces of untreated solid samples (Vickerman and Briggs 2001). It is also a powerful tool to visualise the distribution of chemical components in plant tissues (Aoki et al. 2016a, 2017). A significant advantage of TOF-SIMS over other techniques is its ability to detect molecular or fragment ions of target chemicals and to subsequently visualise their distribution on the sample surface under microscopic lateral resolution. The possibility of a semi-quantitative evaluation of target chemicals was also investigated in the complementary use of quantitative analyses (Zheng et al. 2014a,b, 2016).

The mapping of inorganic metals such as Na, Ca, Mg and Al in dry samples of plants by using TOF-SIMS has been reported (Martin et al. 2004; Tokareva et al. 2007; Saito et al. 2008, 2014). However, during the drying process, as part of the sample preparation, some alterations could occur because of the movement, draining or change in the water-soluble chemicals. The frozen-hydrated plant tissue has the potential to allow biological material to be examined in conditions very similar to the living state; therefore, it is of considerable interest in the field of plant science. Previously, the cryo-TOF-SIMS technique has been used successfully to visualise the inorganic and organic chemicals in freeze-fixed biomaterials with microscopic resolution (Tyler et al. 2006; Metzner et al. 2008, 2010a,b; Iijima et al. 2011; Kuroda et al. 2013; Aoki et al. 2016b, 2017; Jyske et al. 2016).

Hydrangea macrophylla is an Al-tolerant shrub that can accumulate up to 3000 mg kg^{-1} Al in the leaves (DW) (Ma et al. 1997) and approximately 100 mg kg^{-1} fresh weight in the sepals (Toyama-Kato et al. 2003; Ito et al. 2009). The distribution and concentration of inorganic elements in the stem of the species is important for physiology and environmental science. The difference in the distribution of inorganic elements influenced by Al-treatment might help to better understand the Al-tolerance mechanism and reveal the transportation mechanism of inorganic elements in Al-tolerant plants.

In the present study, *H. macrophylla* samples were cultivated with or without $Al_2(SO_4)_3$ administration, and the effect of the Al-treatment was investigated. The cellular distributions of inorganic elements in freeze-dried and -fixed stems of *H. macrophylla* were visualised by dry- and cryo-TOF-SIMS, respectively. Their actual amounts were quantified by inductively coupled plasma atomic emission spectrometry (ICP-AES).

Materials and methods

Material preparation: A cutting of *H. macrophylla* cv. Narumi blue was donated by Okumura Seika-en, Toyoake, Japan and placed on sand. After the root elongated, plants were transferred to pots containing a combination soil (Mikawa Micron Co. Ltd., Toyohashi, Japan) for hydrangeas: AjisaiB1 (pH 4.95 ± 0.12) for Al-treatment and HydrangeaPink (pH 5.29 ± 0.35) for the control (no-treatment). The plants were grown in a greenhouse at Nagoya University (Nagoya, Japan) under the following general conditions: water was absorbed from the bottom of the pot for 30 min daily and the day temperature was controlled around 25°C and that of the night was around 10°C, from July 2014 to May 2015. Half the plants were treated with 500 ml 0.1% (w/v) $Al_2(SO_4)_3$ aqueous solution (Matsunaka 2004) once a month and the others were untreated. Small portions of the stems (approximately 10 mm length, 5 mm diameter) from the native and Al-treated samples were excised speedily with a sharp razor blade and immediately frozen in liquid Freon R22 (DuPont) at –160°C (on June 17, 2015) and stored at –80°C.

Optical microscopy: Thin transverse sections (5 µm thick) were prepared according to the previously reported method for preparing hard tissue sections (Kawamoto and Kawamoto 2014). The sections were stained with safranin and astra blue, or toluidine blue. In plant histochemical staining (Maacz and Vagas 1961), safranin and astra blue are usually sensitive to lignin and polysaccharide, respectively. Toluidine blue, a metachromatic dye, can stain lignified cell walls blue or green, and unlignified cell walls purple (O'Brien et al. 1964). The prepared sections were observed by optical microscopy equipped with polarisers (BX50; Olympus Corp., Tokyo, Japan).

Dry-TOF-SIMS: For each type of sample (native and Al-treated), four frozen sample blocks from three individuals were cut to form a clean and even surface using a sliding microtome (REM-710, Yamato Kohki Industrial Co., Ltd., Saitama, Japan). Then, the samples were freeze-dried, fixed to the sample holder and submitted to dry-TOF-SIMS measurements.

Dry-TOF-SIMS measurements were performed using a TRIFT III spectrometer (ULVAC-PHI, Inc., Kanagawa, Japan). Positive ion spectra were collected under the following conditions: primary ion, 22 keV Au_1^+ at a current of 5 nA; pulse width, 13 ns for unbunched image analysis and 1.8 ns for bunched spectrum analysis. The measured surface areas were 400 × 400 μm^2, and approx. 5×10^6 total ion counts were obtained with an acquisition time of 10 min for each image. A low-energy pulsed electron gun (30.0 eV) was used for surface charge compensation. All square images obtained had 256 × 256 pixels and each pixel corresponded to 1.56 × 1.56 μm^2. Obtained TOF-SIMS images were connected using WinCadence 5.1.2.8 (ULVAC-PHI Inc.) and MatLab R2014a (The MathWorks, Inc., Natick, MA, USA) with PLS Toolbox 7.5.2 (Eigenvector Research, Inc., Manson, WA, USA), and the colour scale was changed by ImageJ software (National Institutes of Health, Bethesda, MD, USA).

Cryo-TOF-SIMS: Two frozen sample blocks of native and Al-treated samples were simultaneously attached to the sample holder with

ice to compare their results under the same conditions. The samples were cut to form a clean and even surface using a sliding microtome at –30°C in the glove box displaced by cooled nitrogen gas. The sample holder was transferred to the cryo-TOF-SIMS by a cryo-vacuum transfer shuttle. The details of the cryo-TOF-SIMS system have been reported previously (Kuroda et al. 2013; Masumi et al. 2014).

The measurement conditions were similar to that of dry-TOF-SIMS and approximately 7×10^6 total ion counts were obtained with an acquisition time of 10 min. The sample stage temperature was maintained at lower than –120°C within the measurements. After the measurements, the sample blocks were used for the preparation of sections for the microscopic observations. Therefore, the sections for microscopic observations were obtained from the same sample blocks for cryo-TOF-SIMS measurements. The observed surfaces for cryo-TOF-SIMS and optical microscopy were nearly the same position in the stem but not the same as each other.

ICP-AES: Approximately 20 mg of native and Al-treated samples were analysed using ICP-AES measurements according to earlier reported methods (Yoshida and Negishi 2013; Mori et al. 2014). Liquid N_2 was added to the frozen samples, then the tissues were crushed using a mortar and pestle, then immersed into 60% HNO_3 aq. at RT for 16 h. The sample suspension was subsequently treated by the wet ashing method under the following conditions: 105°C for 2 h, 160°C for 16 h with 30% H_2O_2 aq. After filtration, the resultant sample solutions were analysed using an ICP instrument (Vista-Pro, Seiko Instruments/Varian Instruments). The concentration of each inorganic metal was quantified using a calibration curve for the standard solution (ICP multi-element standard solution IV, Merck, Germany). Three different frozen blocks were used for an individual. Each type of native and Al-treated sample was collected from three individuals. The resultant data set ($n=9$ for native and Al-treated samples) was used to calculate mean and standard deviation (SD).

Results and discussion

Tissue assignments at the transverse surface of the stem of *H. macrophylla*

The typical stem tissues, mainly the cortex, phloem, cambium, xylem and pith are shown in the transverse sections stained with safranin and astra blue (Figure 1a and c) or with toluidine blue (Figure 1b). The observed transverse sections were not the same as that for the TOF-SIMS measurements; nonetheless, tissue assignments are essential for the advanced evaluation of the *in planta* distribution of inorganic elements. The lignified xylem is narrow, and the almost unlignified cortex and pith are wide (Figure 1). The secondary xylem comprises three types of cells: wood fibres, vessel elements and ray cells (Figure 1a). The primary xylem is located between the secondary xylem and pith (Figure 1b).

In the pith of the stained sections, some spot-like appearances with dark colouration were observed (Figure 1c, arrow). They exhibited extraordinary high birefringence and had a needle-like shape (Figure 1d, arrow). Accordingly, these spot-like appearances in the pith are crystals and will be further discussed with the TOF-SIMS results.

TOF-SIMS spectrum

Figure 2a shows the positive cryo-TOF-SIMS spectrum obtained from the transverse surface of freeze-fixed stem of *H. macrophylla*. Enlarged ion peaks of each inorganic element Na, Mg, Al, K and Ca are also observed (Figure 2b). As shown in Figure 2b, inorganic elements are distinctly separated in the spectrum obtained in a bunched spectrum mode measurement.

Regarding the multivalent ions, the Ca^{2+} ion at m/z 19.98 was slightly observed and the intensity was < 2% of Ca^+ ions at m/z 39.96. The Mg^{2+} ion at m/z 11.99 was indistinguishable because of overlapping with the C^+ ion at m/z 12.00. There were no distinct ion peaks at m/z 13.49 (Al^{2+}) and m/z 8.99 (Al^{3+}).

In this study, a bunched spectrum mode measurement was selected to visualise these inorganic metals because the secondary ion count of Al was low and difficult to separate the m/z 26.98 (Al^{1+}) ion from the next organic ion of m/z 27.02 (C_2H_3) in image mode measurements.

Distribution of inorganic elements in the freeze-dried stem

Figure 3 shows typical dry-TOF-SIMS total ion images in an image (a and b) and bunched spectrum (c and d) mode. Distributions of each inorganic element (e–n) from the bark to pith of both native and Al-treated samples are visualised in a bunched spectrum mode. In the figure, the images on the left side are of the native sample and that on the right are of the Al-treated sample. The annotation of "Max" means the maximum ion count in a pixel in the image. Each image colour scale was independent.

In the total ion images in an image mode (Figure 3a and b), the tissues of the stem are clearly illustrated. The cortex and pith are wide, whereas the xylem with wood fibres, vessel elements, and ray cells is narrow, which is consistent with the results of optical microscopic observations (Figure 1a and b). The boundaries and intracellular details were ambiguous in the bunched spectrum mode images (Figure 3c and d); however, the tissues were distinguishable.

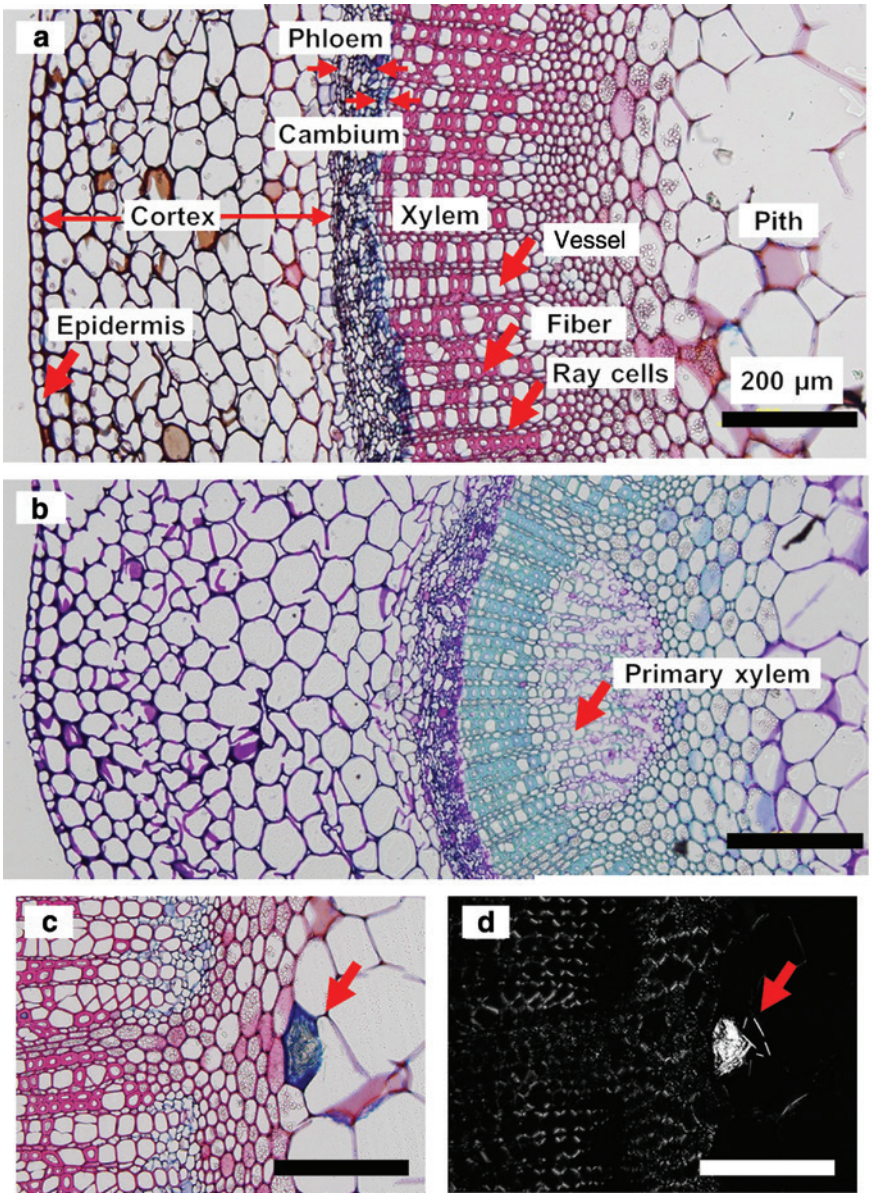

Figure 1: Optical microscopic images of the transverse section of the stem of *Hydrangea macrophylla* stained by (a, c) safranin and astra blue and (b) toluidine blue, (d) was obtained under polarised light, (c) and (d) shown the same position.
Scale bars are 200 μm.

In the native sample, Na was localised mainly in the outer cortex and pith (Figure 3e). After Al-treatment, the Na content of inner cortex increased (Figure 3f). Similar results were observed for Mg (Figure 3g and h) and Ca (Figure 3m and n) distribution.

Al was observed mainly in the inner part of the xylem and outer part of pith in the native sample (Figure 3i). After Al-treatment, Al was distributed more widely, mainly from the inner part of the cortex to xylem (Figure 3j). Al distributions were not similar to that of the other inorganic elements in both sample types.

K was found in all areas from the cortex to the pith in the native sample (Figure 3k). After Al-treatment, the K distribution in xylem decreased (Figure 3l).

The results of dry-TOF-SIMS measurements using freeze-dried samples generally indicated Na, Mg, Al and Ca were found in wide regions in the stem of *H. macrophylla* after the Al-treatment. However, K in the xylem decreased. These results suggest that Al-treatment can alter distribution of not only Al but also other inorganic elements (Na, Mg, K and Ca) in the stem of *H. macrophylla*.

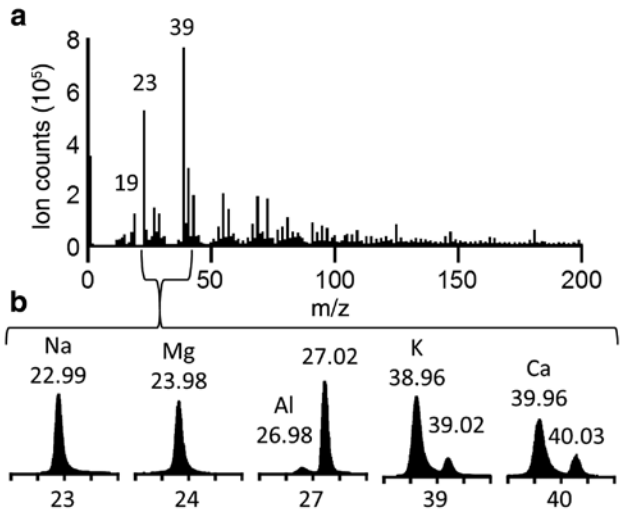

Figure 2: (a) Positive cryo-TOF-SIMS spectrum of the transverse surface of freeze-fixed *Hydrangea macrophylla*.
The spectrum is obtained from the Al-treated sample in a bunched spectrum mode. (b) Enlarged ion peaks of inorganic elements: Na, Mg, Al, K and Ca.

Distribution of inorganic elements in the freeze-fixed stem

Figure 4 shows the cryo-TOF-SIMS total ion images in an image mode (a and b) and in a bunched spectrum mode (c and d). In the total ion images in an image mode (Figure 4a and b), the tissues of the stem are clearly illustrated compared with that of dry-TOF-SIMS. The most important differences should be the intracellular regions. The intracellular regions are vacant in dry-TOF-SIMS but filled in cryo-TOF-SIMS. Distributions of each inorganic element (e–n) from the bark to pith of both native and Al-treated samples are visualised in a bunched spectrum mode. In the figure, the images on the left side are of the native sample and that on the right are of the Al-treated sample.

In the native sample, Na was localised mainly in the middle part of the cortex, cambium and outer part of the pith (Figure 4e). After Al-treatment, the Na content of inner part of cortex and xylem increased (Figure 4f). Mg showed a similar alteration and was detected more frequently in the inner region of the stem after the Al-treatment (Figure 4g and h).

In the inner part of cortex, specific cells showed a high Al content (Figure 4i and j). This phenomenon was not suggested by dry-TOF-SIMS. The possible reason is that the high Al-containing cells in the cortex are limited and the actual amount was relatively low. As a result of the drying process, the focused Al might be scattered. After Al-treatment, Al was more widely distributed (Figure 4j) and the cells containing high levels of Al were still detected.

K was found from the cortex to the outer part of pith in the native sample (Figure 4k). The highest ion counts were found in the cambial region. After Al-treatment, the highest ion count was observed widely in the outer cortex. The K content in the xylem increased relative to that of the control after Al-treatment. However, the colour scale was independent for each image. Regarding the colour alteration in the cortex (green to yellow/red) and xylem (blue to green) after Al-treatment, the relative increment of K detection might be larger in the cortex than that in the xylem.

The Ca content in the xylem, which was mainly localised in the cortex and pith in the native sample (Figure 4m), was rather low. It was distributed narrowly in the inner cortex and pith in the Al-treated sample (Figure 4n). In the pith, a spot-like appearance with a high Ca concentration was detected (Figure 4n). This indicates the presence of calcium oxalate crystals, which commonly appear in living cells in plant tissues (Franceschi and Nakata 2005). This observation confirmed the results of optical microscopy (Figure 1c and d).

In comparison with the dry-TOF-SIMS results, generally, the cell and tissue specific distribution of inorganic elements was visualised in greater detail by cryo-TOF-SIMS using frozen-hydrated samples. The alteration tendency obtained by cryo-TOF-SIMS generally agreed with that suggested by dry-TOF-SIMS. Briefly, Na, Mg, Al and Ca were distributed more in the inner part of the stem after Al-treatment than that of the control. After the Al-treatment, the K distribution might be spread. The difference between dry- and cryo-TOF-SIMS measurements will be discussed further with the quantitative ICP-AES results.

Concentration of inorganic elements in the stem of *Hydrangea macrophylla*

Secondary ion counts in TOF-SIMS measurements strongly depend on the ionisation efficiency of the target chemicals (Vickerman and Briggs 2001). Therefore, the ion counts are not in direct proportion to the actual abundance. In consideration of this point, the actual concentration of inorganic elements was quantified by ICP-AES. The quantification result was compared with the secondary ion counts in dry- and cryo-TOF-SIMS.

The relative intensities of each inorganic element (Na, Mg, Al, K and Ca) normalised to total ions in dry-TOF-SIMS are shown in Figure 5a. The results of four surfaces were used to calculate mean and SD in Figure 5a. Regarding cryo-TOF-SIMS, the combined cryo-TOF-SIMS images were

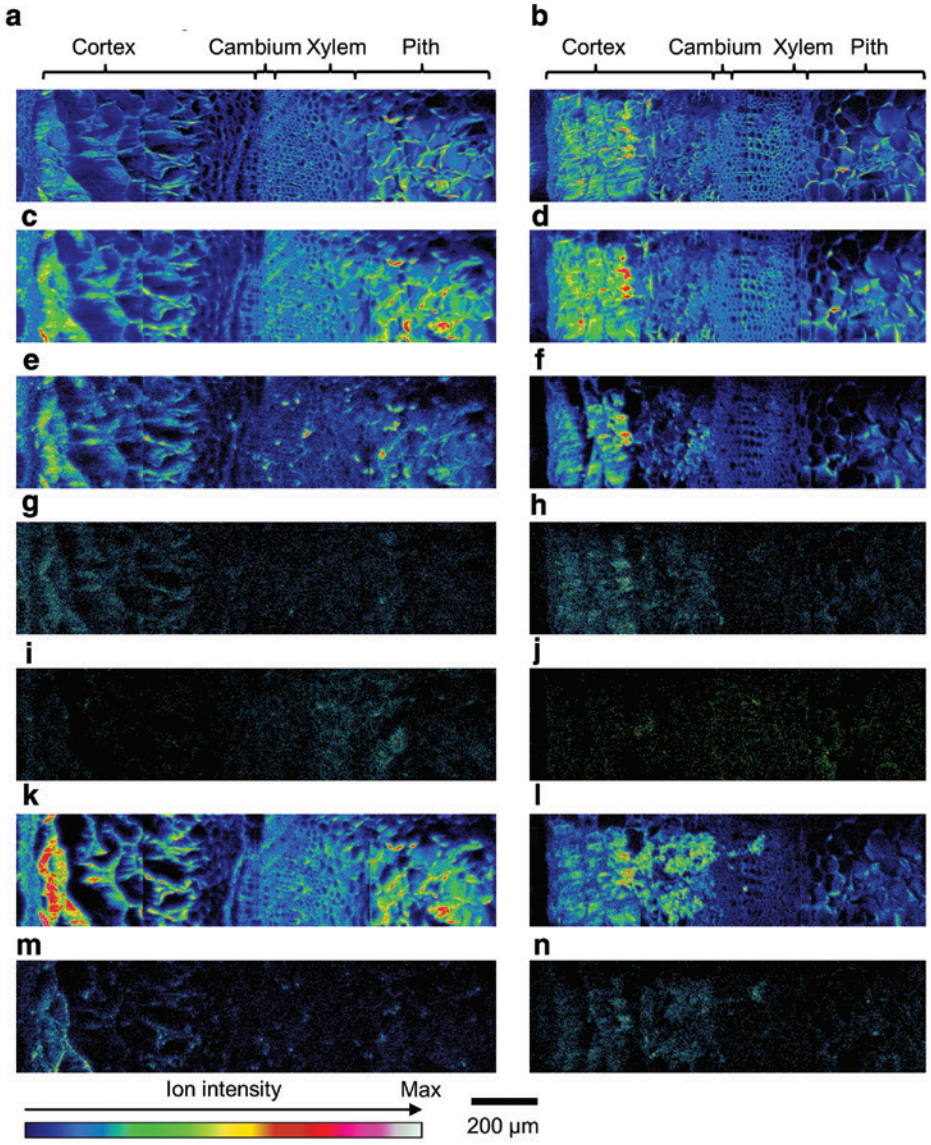

Figure 3: Dry-TOF-SIMS ion images of the transverse surface of freeze-dried stem of *Hydrangea macrophylla*.
The images on the left are of the native sample and those on the right are of the Al-treated sample. Scale bar is 200 μm. Maximum counts per pixel are shown in each image as "Max". (a) Total ion, image mode, Max 1799,(b) total ion, image mode, Max 1065,(c) total ion, spectrum mode, Max 744,(d) total ion, spectrum mode, Max 381, (e) Na^+, Max 37, (f) Na^+, Max 32, (g) Mg^+, Max 6, (h) Mg^+, Max 6, (i) Al^+, Max 5, (j) Al^+, Max 3, (k) K^+, Max 75, (l) K^+, Max 58,(m) Ca^+, Max 12 and (n) Ca^+, Max 6.

divided to four regions of interest (ROIs). For the calculation, each image having 256 pixels in height was divided into 64 pixels in height. The relative intensity of each inorganic element normalised to total ions from every ROI was calculated and shown in Figure 5b. In dry- and cryo-TOF-SIMS measurements, the relative intensities of Mg, Al and Ca were <0.5% and the value was tenfold in Figure 5a and b (shown with 10× magnification). The bulk concentrations of inorganic elements in the stems of native and Al-treated samples were quantified by ICP-AES and are summarised in Figure 5c.

In TOF-SIMS, generally, the secondary ion yield of inorganic metals tends to be related to the elements' preference to gain or lose electrons. Previous research revealed that alkali metals (electropositive elements) readily form positive ions (Heide 2014). It was also reported that the secondary ion yields of alkali metals are one order of magnitude higher than that of alkaline-earth and other metals (Heide 2014). This could explain the lower sensitivity of Mg, Al and Ca than that of Na and K in both dry- and cryo-TOF-SIMS measurements (Figure 5a and b).

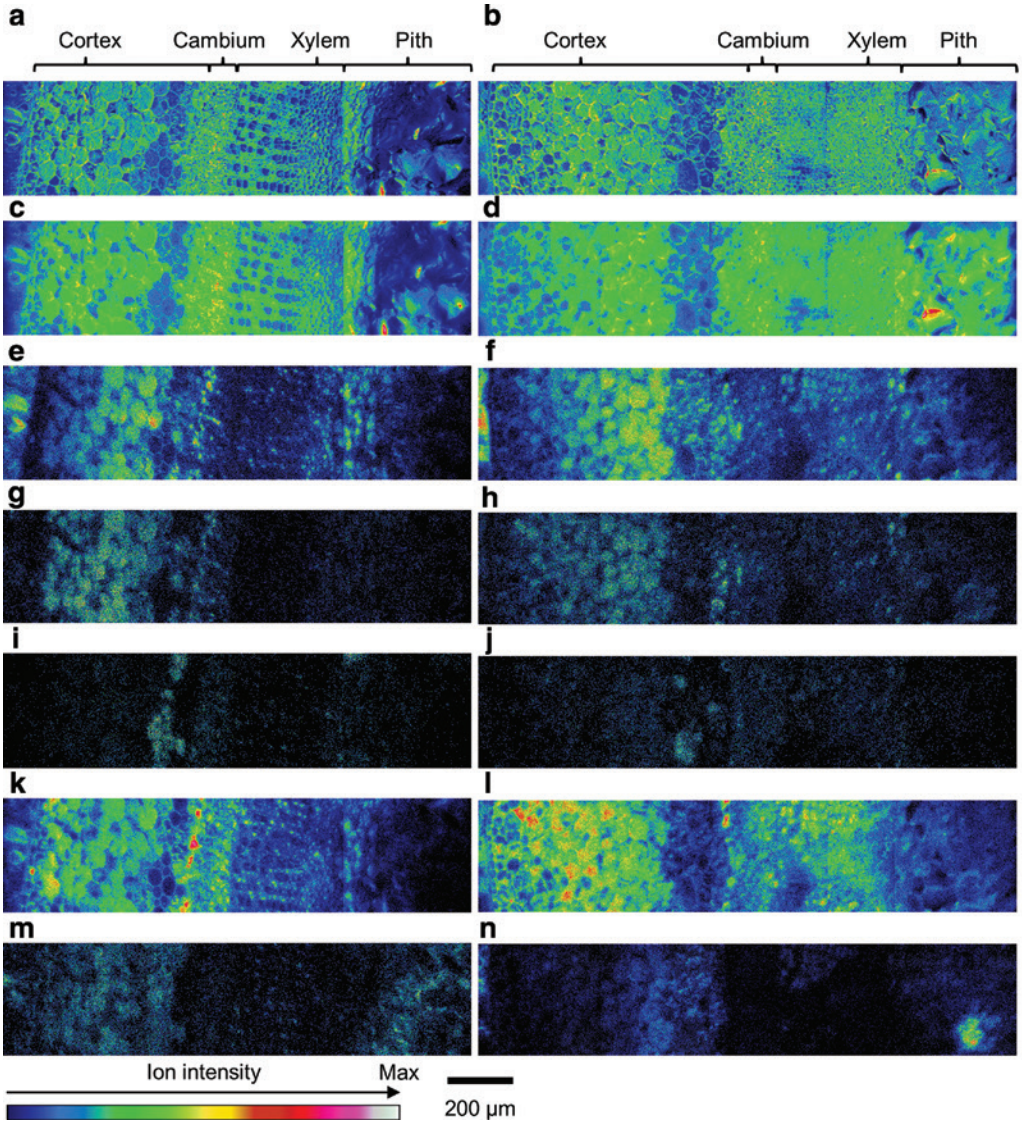

Figure 4: Cryo-TOF-SIMS ion images of the transverse surface of freeze-fixed stem of *Hydrangea macrophylla*.
The images on the left are of the native sample and those on the right are of the Al-treated sample. Scale bar is 200 µm. Maximum counts per pixel are shown in each image as "Max". (a) Total ion, image mode, Max 608, (b) total ion, image mode, Max 945, (c) total ion, spectrum mode, Max 495, (d) total ion, spectrum mode, Max 499, (e) Na^+, Max 29, (f) Na^+, Max 33, (g) Mg^+, Max 10, (h) Mg^+, Max 10, (i) Al^+, Max 6, (j) Al^+, Max 8, (k) K^+, Max 63, (l) K^+, Max 46, (m) Ca^+, Max 9 and (n) Ca^+, Max 27.

In the dry-TOF-SIMS measurement (Figure 5a), after Al-treatment, the relative intensities of Na, Mg and Ca significantly increased ($P < 0.05$) and that of Al increased moderately ($P < 0.1$). However, the relative intensities of K significantly decreased ($P < 0.05$). In the cryo-TOF-SIMS measurements (Figure 5b), the relative intensities of Na, Al and Ca significantly increased, and that of K decreased moderately after Al-treatment. Unexpectedly, the relative intensities of Mg showed almost no difference. Regarding the quantity by ICP-AES, the concentration of Na, Mg, Al and Ca significantly increased and that of K decreased moderately after Al-treatment (Figure 5c).

From these results, the alterations of inorganic elements by Al-treatment were generally consistent between dry-TOF-SIMS and ICP-AES measurements: the concentrations of Na, Mg, Al and Ca increased and that of K decreased after Al-treatment. As for the cryo-TOF-SIMS, although the alteration of Na, Al, K and Ca showed a similar tendency with that of dry-TOF-SIMS, the relative intensity of Mg was different. Cryo-TOF-SIMS measurements showed a detailed distribution of inorganic metals in frozen-hydrated samples; nevertheless, the results should be confirmed further regarding the measurement characteristics.

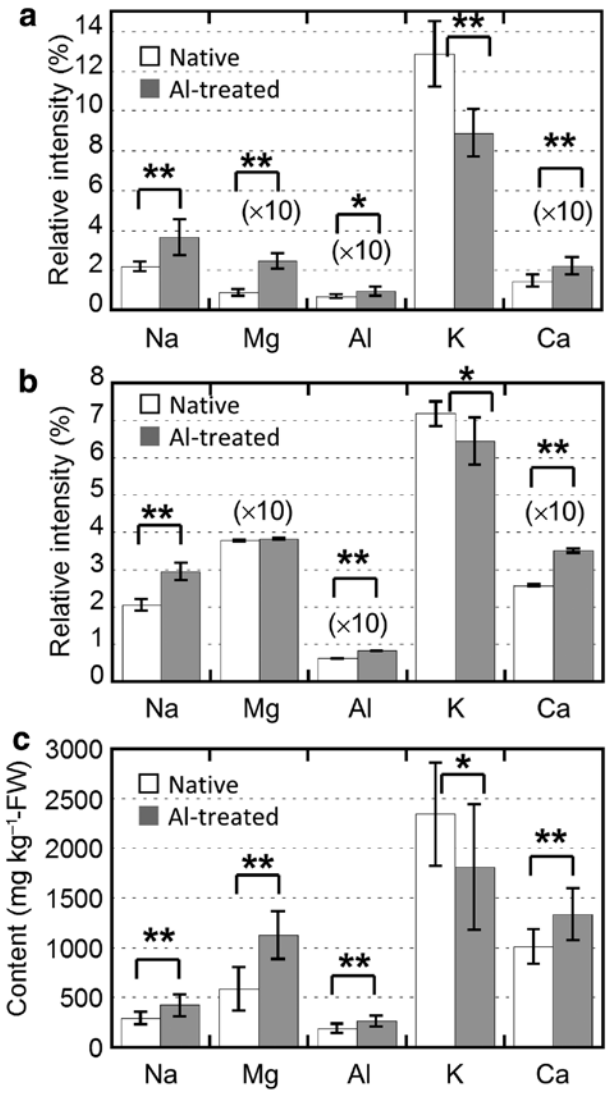

Figure 5: Relative ion intensity of inorganic elements at the transverse surface of (a) freeze-dried stem and (b) freeze-fixed stem of *Hydrangea macrophylla* evaluated by dry-TOF-SIMS ($n = 4$) and cryo-TOF-SIMS ($n = 4$ as ROI), respectively.
The relative intensities of Mg, Al and Ca were tenfold (× 10). (c) The contents of inorganic elements in the stem of *H. macrophylla* evaluated by ICP-AES ($n = 9$). FW, fresh weight. **$P < 0.05$; *$P < 0.1$.

The difference between dry- and cryo-TOF-SIMS measurements should come from their measurement characteristics, i.e. the meaning of the measured surface is different between freeze-dried and frozen-hydrated samples. In this study, dry-TOF-SIMS was used for surface measurements as a result of the concentration of the intracellular content; however, cryo-TOF-SIMS measured only the specific transverse surface of the cell in the freeze-fixed state. Therefore, the intracellular variation of the target chemicals should be considered in the future.

Owing to the direct interference of Al with the efficiency of membrane-transport mechanisms, some inorganic elements (such as Mg and Ca) showed lower internal concentrations in Al-sensitive plants, thereby affecting plant growth (Siegel 1985; Horst 1995; Kochian 1995; Matsumoto 2000; Samac and Tesfaye 2003; Kochian et al. 2004; Ma 2007). The results of the present study showed that the absorption of most inorganic elements (such as Na, Mg, Al and Ca) increased under the influence of Al-treatment in the Al-tolerant plant *H. macrophylla*, which is in disagreement with Al-sensitive plants.

We have previously identified three candidate-genes in *H. hydrangea* involving in Al accumulation (Negishi et al. 2012, 2013). Expression level of *HmVALT*, a tonoplast localised Al-transporter gene, and *HmPALT2*, a plasma-membrane localised Al-transporter gene increased with Al-treatment (unpublished data). Furthermore, *HmPALT2* can transport Fe, Ni, Co, Cd and As (III) as an influx transporter and Zn as an efflux one (Negishi et al. 2013). The characters of these candidate-genes affecting the inorganic metal transportation might affect the mineral balance of the tissue.

Conclusions

The distribution and quantification of inorganic elements (Na, Mg, Al, K and Ca) in freeze-dried and -fixed stems of native and Al-treated *H. macrophylla* were successfully measured by dry-/cryo-TOF-SIMS and ICP-AES. The observed difference between the native and Al-treated samples indicated that the distribution and concentration of various inorganic elements are affected by Al-treatment and suggests flexible inorganic transportation and storage mechanisms in the Al-tolerant plant *H. macrophylla*. The results of both TOF-SIMS and ICP-AES are generally consistent with each other, which shows the possibility of semi-quantitative visualisation of the *in planta* distribution of inorganic elements within a nearly living state. However, although the detection sensitivity and not averaged surface character in the measurements should be considered, the TOF-SIMS measurements are a powerful tool for future studies of the transportation and storage mechanisms of inorganic elements *in planta*.

Acknowledgements: We are grateful to the editors and reviewers for their kind and constructive suggestions. We acknowledge Mr. Seiji Okumura of Okumura Seika-en for donating hydrangeas and Ms. Natsuko Yoshino of Nagoya

University Museum for cultivating hydrangeas. This work was supported by the Japan Society for the Promotion of Science (Nos. 25252032 and 15H01230) and Challenging Exploratory Research (No. 26660014) and Grant-in-Aid for Scientific Research (B) (No. 24380062) from the Ministry of Education, Culture, Sports, Science and Technology, Japan.

References

Aoki, D., Saito, K., Matsushita, Y., Fukushima, K. (2016a) Distribution of cell wall components by TOF-SIMS. In: Secondary Xylem Biology. Eds. Kimi, Y.S., Funada, R., Singh, A.P. Academic Press, New York. pp. 363–379.

Aoki, D., Hanaya, Y., Akita, T., Matsushita, Y., Yoshida, M., Kuroda, K., Yagami, S., Takama, R., Fukushima, K. (2016b) Distribution of coniferin in freeze-fixed stem of *Ginkgo biloba L.* by cryo-TOF-SIMS/SEM. Sci Rep. 6:31525.

Aoki, D., Asai, R., Tomioka, R., Matsushita, Y., Asakura, H., Tabuchi, M., Fukushima, K. (2017) Translocation of ^{133}Cs administered to *Cryptomeria japonica* wood. Sci. Total Environ. 584–585:88–95.

Famoso, A.N., Clark, R.T., Shaff, J.E., Craft, E., McCouch, S.R., Kochian, L.V. (2010) Development of a novel aluminum tolerance phenotyping platform used for comparisons of cereal aluminum tolerance and investigations into rice aluminum tolerance mechanisms. Plant Physiol. 153:1678–1691.

Franceschi, V.R., Nakata, P.A. (2005) Calcium oxalate in plants: formation and function. Annu Rev Plant Biol. 56:41–71.

Hajiboland, R., Rad, S.B., Barceló, J., Poschenrieder, C. (2013) Mechanisms of aluminum-induced growth stimulation in tea (*Camellia sinensis*). J. Plant Nutr. Soil Sci. 176:616–625.

Heide, P. (2014) Principles. In: Secondary Ion Mass Spectrometry: An Introduction to Principles and Practices. Eds. Heide, P. John Wiley & Sons, Inc., Hoboken, NJ. pp. 23–138.

Horst, W.J. (1995) The role of the apoplast in Aluminum toxicity and resistance of higher-plants: A review. Z. Pflanz. Bodenkunde 158:419–428.

Iijima, M., Yoshida, T., Kato, T., Kawasaki, M., Watanabe, T., Somasundaram, S. (2011) Visualization of lateral water transport pathways in soybean by a time of flight-secondary ion mass spectrometry cryo-system. J. Exp. Bot. 62:179–2188.

Ito, D., Shinkai, Y., Kato, Y., Kondo, T., Yoshida, K. (2009) Chemical studies on different color development in blue- and red-colored sepal cells of *Hydrangea macrophylla*. Biosci. Biotech. Biochem. 73:1054–1059.

Jyske, T., Kuroda, K., Suuronen, J.P., Pranovich, A., Roig-Juan, S., Aoki, D., Fukushima, K. (2016) *In planta* localization of stilbenes within *Picea abies* phloem. Plant Physiol. 172:913–928.

Kawamoto, T., Kawamoto, K. (2014) Preparation of thin frozen sections from nonfixed and undecalcifled hard tissues using Kawamoto's Film Method (2012). In: Skeletal Development and Repair: Methods and Protocols. Ed. Hilton, M.J. Human Press, Springer Science+Business Media, New York, NY. pp. 149–164.

Kochian, L.V., Hoekenga, O.A., Pineros, M.A. (2004) How do crop plants tolerate acid soils? Mechanisms of aluminum tolerance and phosphorous efficiency. Annu. Rev. Plant Biol. 55:59–493.

Kochian, L.V. (1995) Cellular mechanisms of aluminum toxicity and resistance in plants. Annu. Rev. Plant Phys. 46:237–260.

Kuroda, K., Fujiwara, T., Imai, T., Takama, R., Saito, K., Matsushita, Y., Fukushima, K. (2013) The cryo-TOF-SIMS/SEM system for the analysis of the chemical distribution in freeze-fixed *Cryptomeria japonica* wood. Surf. Interface Anal. 45:215–219.

Ma, J.F. (2007) Syndrome of aluminum toxicity and diversity of aluminum resistance in higher plants. Int. Rev. Cytol. 264:225–252.

Ma, J.F., Hiradate, S., Nomoto, K., Iwashita, T., Matsumoto, H. (1997) Internal detoxification mechanism of Al in hydrangea. Plant Physiol. 113:1033–1039.

Ma, J.F., Ryan, P.R., Delhaize, M. (2001) Aluminium tolerance in plants and the complexing role of organic acids. Trends Plant Sci. 6:273–278.

Maacz, G.J., Vagas, E. (1961) A new method for staining of cellulose and lignified cell-walls. Mikroskopie 16:40–43.

Martin, R.R., Naftel, S.J., Macfie, S., Skinner, W., Courchesne, F., Seguin, V. (2004) Time of flight secondary ion mass spectrometry studies of the distribution of metals between the soil, rhizosphere and roots of *Populus tremuloides* Minchx growing in forest soil. Chemosphere 54:1121–1125.

Masumi, T., Matsushita, Y., Aoki, D., Takama, R., Saito, K., Kuroda, K., Fukushima, K. (2014) Adsorption behavior of poly (dimethyldiallylammonium chloride) on pulp fiber studied by cryo time-of-flight secondary ion mass spectrometry and cryo-scanning electron microscopy. Appl. Surf. Sci. 289:155–159.

Matsumoto, H. (2000) Cell biology of aluminum toxicity and tolerance in higher plants, Int. Rev. Cytol. 200:1–46.

Matsunaka, T. (2004) Dojougaku no Kiso. Nousangyoson Bunka Kyokai, Tokyo. pp. 136–139 (In Japanese).

Metzner, R., Schneider, H.U., Breuer, U., Schroeder, W.H. (2008) Imaging nutrient distributions in plant tissue using time-of-flight secondary ion mass spectrometry and scanning electron microscopy. Plant Physiol. 147:1774–1787.

Metzner, R., Schneider, H.U., Breuer, U., Thorpe, M.R., Shurr, U., Shroeder, W.H. (2010a) Tracing cationic nutrients from xylem into stem tissue of French bean by stable isotope tracers and cryo-secondary ion mass spectrometry. Plant Physiol. 152:1030–1043.

Metzner, R., Thorpe, M.R., Breuer, U., Blümler, P., Shurr, U., Schneider, H.U., Schroeder, W.H. (2010b) Contrasting dynamics of water and mineral nutrients in stems shown by stable isotope tracers and cryo-SIMS. Plant Cell Environ. 33:1393–1407.

Mori, M., Miki, N., Ito, D., Kondo, T., Yoshida, K. (2014) Structure of tecophilin, a tri-caffeoylanthocyanin from the blue petals of *Tecophilaea cyanocrocus*, and the mechanism of blue color development. Tetrahedron 70:8657–8664.

Negishi, T., Oshima, K., Hattori, M., Kanai, M., Mano, S., Nishimura, M., Yoshida, K. (2012) Tonoplast- and plasma membrane-localized aquaporin-family transporters in blue hydrangea sepals of aluminum hyperaccumulating plant. PLoS One 7:e43189.

Negishi, T., Oshima, K., Hattori, M., Yoshida, K. (2013) Plasma membrane-localized Al-transporter from blue hydrangea sepals is a member of the anion permease family. Genes Cells 18:341–352.

O'Brien, T.P., Feder, N., McCully, M.E. (1964) Polychromatic staining of plant cell walls by toluidine blue O. Protoplasma 59:368–373.

Rout, G.R., Samantaray, S., Das, P. (2001) Aluminium toxicity in plants: a review. Agronomie 21:3–21.

Rufty, T.W., Mackown, C.T., Lazof, D.B., Carter, T.E. (1995) Effects of aluminum on nitrate uptake and assimilation. Plant Cell Environ. 18:1325–1331.

Saito, K., Mitsutani, T., Imai, T., Matsushita, Y., Yamamoto, A., Fukushima, K. (2008) Chemical differences between sapwood and heartwood of *Chamaecyparis obtuse* detected by ToF-SIMS. Appl. Surf. Sci. 255:1088–1091.

Saito, K., Watanabe, Y., Matsushita, Y., Imai, T., Koike, T., Sano, Y., Funada, R., Fukazawa, K., Fukushima, K. (2014) Aluminum localization in the cell walls of the mature xylem of maple tree detected by elemental imaging using time-of-flight secondary ion mass spectrometry (TOF-SIMS). Holzforschung 68:85–92.

Samac, D.A., Tesfaye, M. (2003) Plant improvement for tolerance to aluminum in acid soils: A review. Plant Cell Tiss. Org. 75:189–207.

Schmitt, M., Boras, S., Tjoa, A., Watanabe, T., Jansen, S. (2016) Aluminium accumulation and intra-tree distribution patterns in three *Arbor aluminosa* (Symplocos) species from central Sulawesi. PLoS One 11:e0149078.

Shen, R.F., Chen, R.F., Ma, J.F. (2006) Buckwheat accumulates aluminum in leaves but not in seeds. Plant Soil 284:265–271.

Siegel, N. (1985) Aluminum interaction with biomolecules: the molecular basis for aluminum toxicity. Am. J. Kidney Dis. 6:353–357.

Tokareva, E.N., Pranovich, A.V., Fardim, P., Daniel, G., Holbom, B. (2007) Analysis of wood tissues by time-of-flight secondary ion mass spectrometry. Holzforschung 61:647–655.

Toyama-Kato, Y., Yoshida, K., Fujimori, E., Haraguchi, H., Shimizu, Y., Kondo, T. (2003) Analysis of metal elements of hydrangea sepals at various growing stages by ICP-AES. Biochem. Eng. J. 14:237–241.

Tyler, B.J., Rangaranjan, S., Moller, J., Beumer, A., Arlinghaus, H.F. (2006) TOF-SIMS imaging of chlorhexidine-digluconate transport in frozen hydrated biofilms of the fungus *Candida albicans*. Appl. Surf. Sci. 252:6712–6715.

Vickerman, J.C., Briggs, D. TOF-SIMS: Surface analysis by Mass Spectrometry. IM Publications and Surface Spectra Limited, West Sussex, U.K, 2001.

Vonuexkull, H.R., Mutert, E. 1995. Global extent, development and economic-impact of acid soils. Plant Soil 171:1–15.

Watanabe, T., Misawa, S., Hiradate, S., Osaki, M. (2008a) Root mucilage enhances aluminum accumulation in *Melastoma malabathricum*, an aluminum accumulator. Plant Signal. Behav. 3:603–605.

Watanabe, T., Misawa, S., Hiradate, S., Osaki, M. (2008b) Characterization of root mucilage from *Melastoma malabathricum*, with emphasis on its roles in aluminum accumulation. N. Phytol. 178:581–589.

Yoshida, K., Negishi, T. (2013) The identification of a vacuolar iron transporter involved in the blue coloration of cornflower petals. Phytochemistry 94:60–67.

Zheng, P., Aoki, D., Yoshida, M., Matsushita, Y., Imai, T., Fukushima, K. (2014a) Lignification of ray parenchyma cells in xylem of *Pinus densiflora*. Part I: Microscopic investigation by POM, UV microscopy, and TOF-SIMS. Holzforschung 68:897–905.

Zheng, P., Aoki, D., Matsushita, Y., Yagami, S., Fukushima, K. (2014b) Lignification of ray parenchyma cells in the xylem of *Pinus densiflora*. Part II: Microchemical analysis by laser microdissection and thioacidolysis. Holzforschung 68: 907–913.

Zheng, P., Aoki, D., Matsushita,Y., Yagami, S., Sano, Y., Yoshida, M., Fukushima, K. (2016) Lignification of ray parenchyma cells (RPCs) in the xylem of *Phellodendron amurense* Rupr.: quantitative and structural investigation by TOFSIMS and thioacidolysis of laser microdissection cuts of RPCs. Holzforschung 70:641–652.